Re-expression of alpha skeletal actin as a marker for dedifferentiation in cardiac pathologies

Ronald B. Driesen [a], Fons K. Verheyen [a], Wiel Debie [a], Erik Blaauw [b], Fawzi A. Babiker [b],
Richard N.M. Cornelussen [b], Jannie Ausma [b], Marie-Hélène Lenders [a], Marcel Borgers [a],
Christine Chaponnier [c], Frans C. S. Ramaekers [a], *

[a] *Department of Molecular Cell Biology, Maastricht University, Maastricht, The Netherlands*
[b] *Department of Physiology, CARIM-School for Cardiovascular Diseases, Maastricht University, Maastricht, The Netherlands*
[c] *Department of Pathology and Immunology, Faculty of Medicine, University of Geneva, Geneva, Switzerland*

Abstract

Differentiation of foetal cardiomyocytes is accompanied by sequential actin isoform expression, *i.e.* down-regulation of the 'embryonic' alpha smooth muscle actin, followed by an up-regulation of alpha skeletal actin (αSKA) and a final predominant expression of alpha cardiac actin (αCA). Our objective was to detect whether re-expression of αSKA occurred during cardiomyocyte dedifferentiation, a phenomenon that has been observed in different pathologies characterized by myocardial dysfunction. Immunohistochemistry of αCA, αSKA and cardiotin was performed on left ventricle biopsies from human patients after coronary bypass surgery. Furthermore, actin isoform expression was investigated in left ventricle samples of rabbit hearts suffering from pressure- and volume-overload and in adult rabbit ventricular cardiomyocytes during dedifferentiation *in vitro*. Atrial goat samples up to 16 weeks of sustained atrial fibrillation (AF) were studied ultrastructurally and were immunostained for αCA and αSKA. Up-regulation of αSKA was observed in human ventricular cardiomyocytes showing down-regulation of αCA and cardiotin. A patchy re-expression pattern of αSKA was observed in rabbit left ventricular tissue subjected to pressure- and volume-overload. Dedifferentiating cardiomyocytes *in vitro* revealed a degradation of the contractile apparatus and local re-expression of αSKA. Comparable αSKA staining patterns were found in several areas of atrial goat tissue during 16 weeks of AF together with a progressive glycogen accumulation at the same time intervals. The expression of αSKA in adult dedifferentiating cardiomyocytes, in combination with PAS-positive glycogen and decreased cardiotin expression, offers an additional tool in the evaluation of myocardial dysfunction and indicates major changes in the contractile properties of these cells.

Keywords: hibernation • arrhythmia • heart failure • contractile apparatus • myocytes

Introduction

Alpha cardiac actin (αCA) and alpha skeletal actin (αSKA) are the major sarcomeric actin isoforms detected in striated muscle [1, 2]. A sequential activation of alpha actin isoforms has been demonstrated in several species during the development of the heart [3–7]. The expression of alpha smooth muscle actin (αSMA) marks the earliest appearance of embryonic cardiomyocytes, preceding the co-expression of αSKA and αCA in the developing myocardium, and finally the predominant expression of αCA in the

adult heart [3]. The expression pattern of actin isoforms varies between species and is highly influenced by pathological conditions [8]. Increased αSKA expression represents a well-accepted marker for cardiac hypertrophy in different animal species and man [6, 9–12]. Skeletal actin mRNA accumulation is observed during hemodynamic overload of rat hearts [10, 13], during passive stretch [14] and after administration of compounds such as α1-adrenergic agonists [15], TGF-β1 or bFGF [16] to cultured neonatal rat cardiomyocytes.

The re-expression of αSMA is used as a marker for cardiomyocyte dedifferentiation in cardiovascular diseases characterized by myocardial hibernation [17, 18]. Hibernating cardiomyocytes show typical cellular alterations such as a redistribution of nuclear heterochromatin, depletion of sarcomeres, aberrantly shaped but viable mitochondria and degradation of structured

*Correspondence to: Frans C.S. RAMAEKERS,
Ph.D., Department of Molecular Cell Biology (Box 17),
University of Maastricht, P.O. Box 616, 6200 MD Maastricht,
The Netherlands.
Tel.: +31-433881351; Fax: +31-433884151
E-mail: f.ramaekers@molcelb.unimaas.nl*

sarcoplasmic reticulum in the cardiomyocytes [19–21]. The expression pattern of several structural proteins resembles that of embryonic and foetal cardiomyocytes. For example, the highly organized patterns of cardiotin, titin and desmin disappear or change and there is an increased deposition of glycogen. The structural adaptations have been coined as features of programmed cell survival, a general phenomenon encountered in various pathological situations as in ischaemia-related chronic hibernating myocardium [22], infarction border zones [18, 23] and volume-overloaded myocardium [24].

A goat model of sustained atrial fibrillation (AF) has previously been developed [17] in which structural changes in the myocardial cells are comparable to those observed in hibernating myocardium in man. This model provides the opportunity to study sarcomeric remodelling in more detail at fixed time-points during AF.

The aim of the present study was to investigate the expression patterns of αSKA in human left ventricle samples characterized by chronic hibernating myocardium and in experimental models of cardiac pathologies. Actin staining patterns of left ventricle samples taken from pressure- and volume-overloaded rabbit hearts were compared to atrial samples of chronic AF in goats in which a time-related up- and down-regulation of αSKA was observed during 16 weeks of AF. In addition, the changes in expression of αSKA in cultured adult rabbit ventricular cardiomyocytes, and the relation with the presence of αCA stress fibres during the dedifferentiation process are being discussed.

Materials and methods

All experimental procedures and protocols were carried out according to the Dutch Law on Animal Experimentation (WOD) and approved by the Animal Investigation Committee of Maastricht University. The investigation conforms to the Guide for the Care and Use of Laboratory animals published by the US National Institutes of Health (NIH Publication No. 85–23 revised 1996). All human patients gave their informed consent and the study was approved by the local ethical committees for research. The investigation conforms with the principles outlined in the Declaration of Helsinki. Detailed information on the myocardial samples and the immunocytochemical procedures can be found in the supplementary data section.

Production and characterization of antibodies

Mouse monoclonal anti-α-skeletal actin (anti-αSKA) and anti-α-cardiac actin (anti-αCA) antibodies were prepared following the Repetitive Immunizations at Multiple Sites strategy (RIMMS) [25]. Mice were immunized with the N-terminal nonapeptide of αSKA (Ac-DEDETTALVC-COOH) or αCA (Ac-DDEETTALVC-COOH) conjugated with keyhole limpet haemocyanin (KLH, Pierce, Thermo Scientific, IL, USA) through the cysteine residue according to the instructions of the manufacturer. Lymphocytes from lymph nodes isolated from the immunized mice were fused with NS0 myeloma cells. Hybridoma cells secreting anti-αSKA or anti-αCA were screened by ELISA, Western blotting and immunocytochemical procedures. Selected hybridomas were cloned twice by limited dilution, and the

final characterization of the antibodies was performed by immunoblotting of one-dimensional gels containing tissue and cell extracts.

Characterization and specificity of the cardiotin antibody has previously been described. It was shown that cardiotin is associated with cardiac mitochondria, and is down-regulated gradually during cardiomyocyte dedifferentiation [17, 26–28].

Gel electrophoretic and immunoblot analysis

Anti-α-SKA and anti-α-CA specificity was determined by immunoblotting of the following whole tissue homogenates: rat aorta, rat myocardium, rat-striated muscle, human platelets and chicken gizzard (2 μg/lane). Sodium dodecyl sulfate-polyacrylamide gel electrophoresis (SDS-PAGE) was carried out in 10% polyacrylamide gels and proteins were consequently electroblotted to nitrocellulose membranes. These blots were incubated with anti-α-SKA and anti-α-CA diluted in Tris-buffered saline solution (TBS) containing 3% BSA and 0.1% Triton X-100 for 2 hrs at room temperature. After 3 washes with TBS, a second incubation was performed with peroxidase-conjugated affinity purified goat anti-mouse IgG (Jackson Immunoresearch Laboratories, West Grove, PA, USA) at a dilution of 1:10,000 in TBS containing 0.1% BSA and 0.1% Triton X-100. A pan-actin monoclonal antibody (clone C4, Chemicon, Temecula, CA, USA) was used for normalization. Peroxidase activity was developed using the ECL Western blotting system (GE Healthcare, Munich, Germany), according to the instructions of the manufacturer and blots were scanned (Epson Perfection 4990 Photo, Epson Deutschland GmbH Meerbusch, Germany) and quantified using densitometric analysis (Optiquant software; Packard Instrument Co., Meriden, CT, USA).

Myocardial tissue samples

Human coronary artery disease.
The human cardiac material used in this study consisted of transmural left ventricle biopsies from 4 patients obtained during coronary artery bypass surgery. The detailed individual patient characteristics are described in previous papers [19, 21, 22]. Left ventricle biopsies were directly frozen in isopentane precooled with liquid nitrogen.

Pressure- and volume-overload of rabbit hearts.
Aortic valve insufficency and aortic banding was induced in 4 adult female white New Zealand rabbits as described previously [29] and compared to a group of 5 sham-operated rabbits without aortic interventions. The rabbits were bred and housed under specified pathogen-free conditions. The excised left ventricles were immediately frozen in liquid nitrogen-precooled isopentane and used for light microscopy and immunohistochemistry.

Chronic atrial fibrillation in goats.
The goat model for chronic AF was described previously [30]. In total, 22 goats were used in this study. The control group (2 animals) was kept in sinus rhythm, whereas in the other groups (3–4 goats/group) AF was maintained for 1, 2, 4, 8 and 16 weeks, respectively. At the end of the experimental period, the goats were anaesthetized and thoracotomy was performed. The excised right and left appendages were immediately frozen in liquid nitrogen-precooled isopentane and used for light microscopy and immunohistochemistry. The material examined in this study was previously studied for an extensive series of dedifferentiation markers [17].
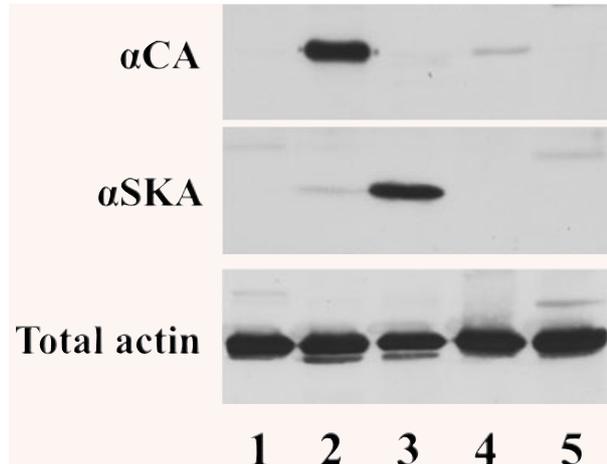
Fig. 1 Characterization of anti-αSKA and anti-αCA by immunoblotting on different tissue or cell extracts: rat aorta (lane 1), rat myocardium (lane 2), rat skeletal muscle (lane 3), human platelets (lane 4) and chicken gizzard (lane 5). A pan-actin antibody (total actin) was used for normalization.

Histological analysis

Light microscopic examination of the morphologic changes was performed on 5-μm thick cryosections of rabbit ventricular and goat atrial tissue stained with periodic acid Schiff (PAS) to localize the glycogen content and counterstained with Mayers haematoxylin (Klinipath, the Netherlands). Indirect immunofluorescence assays were performed on 5-μm thick cryosections of human, goat and rabbit myocardial tissue. Goat and rabbit sections were incubated separately with the primary antibodies against αSKA (mouse monoclonal IgM) or αCA (mouse monoclonal IgG) and human sections were incubated simultaneously for αCA and αSKA. Serially sectioned human samples were also incubated with a primary antibody against cardiotin (R2G anti-cardiotin mouse IgM antibody). Nuclei were routinely stained with 4'-6-diamidine 2-o-phenylindole (DAPI), diluted 1:10,000 (Sigma Chemicals, St. Louis, MO, USA).

Cell isolation

New Zealand White rabbits (ca. 2 kg) were used for the generation of myocard cell cultures. Cardiomyocytes and cardiac fibroblasts were isolated from adult rabbits by a retrograde collagenase perfusion as previously described [31]. The cells were seeded on laminin-coated (10 μg/ml; Life Technologies, Paisley, Scotland) glass bottom microwell dishes (MatTek Corporation, Ashland, MA, USA) or cover glasses in petri dishes at a low density (10^3 cells/ cm^2) to avoid cell–cell contact. Cells were allowed to attach for 2 hrs. Thereafter, fresh medium supplemented with 20% foetal bovine serum (Hyclone, Logan, UT, USA) was applied onto the cells. Cells were kept in a humidified incubator (5% CO_2, 37°C) and the medium was replaced every other day. Because of their high proliferative capacity, rabbit cardiac fibroblasts could be passaged up to 6 times using 0.05% trypsin-EDTA (Life Technologies). Cardiac fibroblasts were added to the cardiomyocytes in a 1:1 ratio 1 day after suspending in Medium 199 in order to accelerate the dedifferentiation process [32].

Immunocytochemistry of cultured cells

Separate cover glasses were processed either 3 hrs after seeding (day 0), or on subsequent days ranging from day 1 to day 5 after seeding. The medium was discarded and the cells were rinsed with phosphate buffered saline (PBS). Before immunostaining for αSKA, the cells were fixed in −20°C methanol (3 × 1 sec.) and aceton (1 sec.), air dried and frozen at −20°C until further use. For optimal detection of αCA immunostaining, fibroblast−cardiomyocyte co-cultures were fixed in 4% paraformaldehyde in PBS for 20 min., autofluorescence was quenched with 0.05 M NH₄Cl for 45 min. and incubated in 0.05% Nonidet P40 in PBS during 30 min. Coverslips were mounted with glycerol containing 0.2 μg/ml propidium iodide. Double-staining of αCA and αSKA was performed according to the previously described protocol in the section of the histological analysis.

Confocal scanning laser microscopy

Fluorescent samples of single stained cell cultures were imaged using a Bio-Rad MRC600 confocal microscope (Bio-Rad Laboratories Ltd, Hemel Hempstead, UK), equipped with an air-cooled Argon–Krypton mixed gas laser and mounted onto an Axiophote microscope (Zeiss, Oberkochen, Germany), using oil-immersion objectives (40×, NA 3D1.3 or 63×, NA 3D1.4). Fluorescent pictures are depicted as total z-stack images.

Electron microscopy

For transmission electron microscopy, rabbit cardiomyocyte cultures and goat atrial samples were fixed in 3% glutaraldehyde buffered with 90 mM KH_2PO_4, pH 7.4, After rinsing in the same buffer for 24 hrs, the samples were postfixed for 1 hr in 2% OsO_4 (Agar Scientific, Stansted, UK) buffered to pH 7.4 with 0.1 M veronalacetate. Additional impregnation of cardiomyocyte cultures was performed in 1% uranylacetate (LADD Research Industries, Burlington, VT, USA) in 0.1 M veronalacetate, pH 5.2. The cardiomyocyte cultures and atrial samples were dehydrated in graded series of ethanol and routinely embedded in Epon (LADD Research Industries). Semi-thin sections of atrial samples were stained with PAS and toluidin blue for light microscopical evaluation. Ultrathin sections were counterstained with uranylacetate and lead citrate, prior to examination in a Philips CM100 electron microscope.

Results

Specificity of actin antibodies

Western blot analysis of the αCA and αSKA mouse monoclonal antibodies on respectively rat aorta, rat myocardium, rat skeletal muscle, human platelets and chicken gizzard revealed a strong specificity of αCA for rat myocardium and αSKA for rat skeletal muscle (Fig. 1). From these results, it becomes obvious that both monoclonal antibodies do not cross-react with the α- and γ-smooth muscle actin isoforms present in the aorta
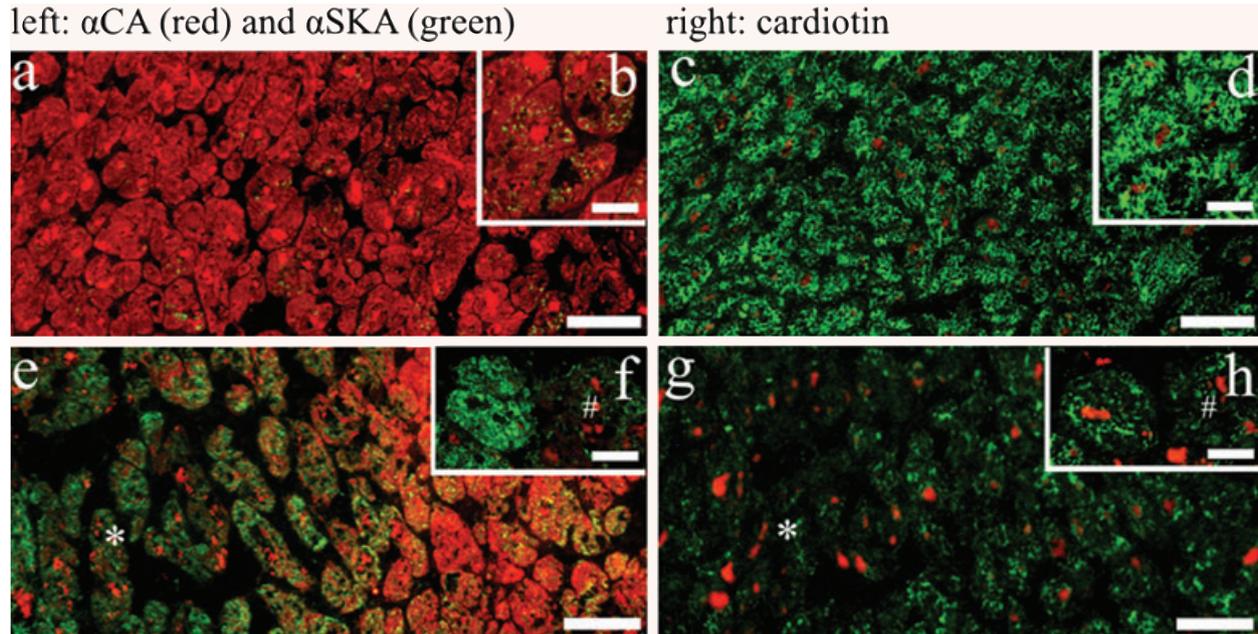
Fig. 2 Detection of αCA (**A, B, E, F**, red), αSKA (**A, B, E, F**, green) and cardiotin (**C, D, G, H**, green) on serial frozen sections from human left ventricular endocardial biopsies after coronary bypass surgery. Control region showing normal expression of αCA (**A, B**, red) and cardiotin (**C, D**, green) with only minor expression of αSKA (**B**, green). The hibernating region (asterisk) shows increased αSKA staining (**E**, green), whereas αCA (**E**) and cardiotin (**G**) expression is nearly absent. Inserts (**F** and **H**) depict two serially sectioned cardiomyocytes present in a hibernating area: the left cardiomyocyte shows an apparent up-regulation of αSKA (**F**), absence of αCA (**F**) and down-regulation of cardiotin (**H**), the right cardiomyocyte (#) is nearly negative for both actins as well as cardiotin. Lipofuscin granules in the sections show an orange autofluorescence signal. Scale bars represent 20 μm (**A, C, E, G**) and 50 μm (**B, D, F, H**).

and gizzard samples, nor with the cytoplasmic β- and γ-actin isoforms present in the platelet sample. Also, no cross-reactivity of the αCA is observed with α-skeletal actin, nor of the αSKA with α-cardiac actin.

The peptide sequences to which these two antibodies are directed are strongly conserved during evolution, resulting in a reactivity with striated muscle actins from a wide spectrum of animal species.

Ventricular hibernating myocardium in man

The larger part of the left ventricular tissue of patients suffering from coronary artery disease showed normal αCA (Fig. 2A and B) and cardiotin expression (Fig. 2C and D). Some of the cardiomyocytes revealed a minor punctate expression pattern of αSKA in their cytoplasm (Fig. 2A and B). Twenty to 45% of the total tissue area revealed a strong re-expression of αSKA. Several of the affected cells demonstrated an intense patchy localization of αSKA (Fig. 2E and F) with a concomitant down-regulation of αCA (Fig. 2E and F) and cardiotin (Fig. 2G and H). Furthermore, absence of αSKA (Fig. 2F) and cardiotin (Fig. 2H) was observed in αCA weak positive cardiomyocytes (Fig. 2F) in other regions of the same sections.

Pressure- and volume-overloaded rabbit hearts

Longitudinal sections of left ventricle tissue of sham-operated rabbits revealed a normal αCA cross-striated pattern in the cardiomyocytes (Fig. 3A). The tissue was devoid of any αSKA expression (Fig. 3C) and the PAS staining showed no glycogen deposition (Fig. 3E). After 16 weeks of overload, αCA was still abundantly expressed (Fig. 3B) but some regions demonstrated an intense patchy expression of αSKA (between 20% and 40% of total tissue area) (Fig. 3D). PAS staining of the αSKA-positive regions often showed an accumulation of glycogen (Fig. 3F), although not all areas with αSKA-positive cardiomyocytes were PAS-positive.

Actin re-organization in cultured adult rabbit cardiomyocytes

In a previous *in vitro* study, we have classified the progressive phenotypic adaptations of rabbit cardiomyocytes into 5 consecutive groups (Groups 1 to 5) [32]. Approximately 3 hrs after isolation, the cardiomyocytes showed still intact sarcomeric cross-striations with staircase-like distal ends of the cell (non-differentiated Group 0 cardiomyocytes, Fig. 4A). The first change after 1 day in culture was a rounding up of the distal ends (Group 1, Fig. 4B), followed
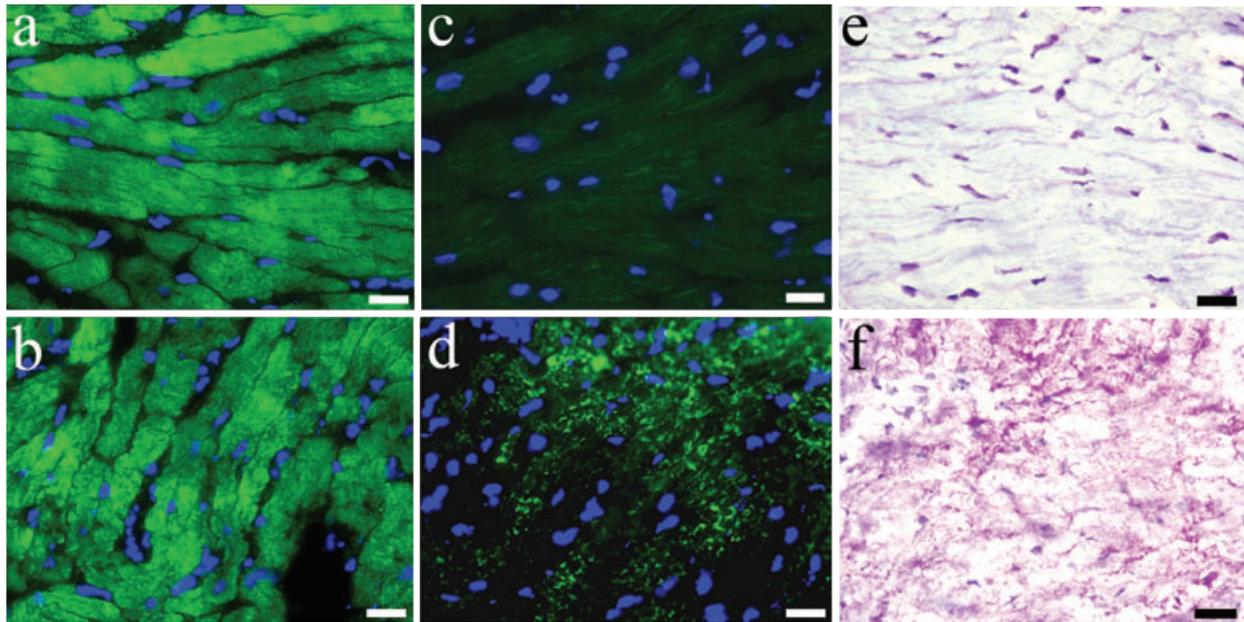
Fig. 3 Detection of αCA (**A, B**), αSKA (**C, D**) and periodic acid Schiff (PAS) staining (**E, F**) in frozen sections from sham left rabbit ventricular myocardium (**A, C, E**) and left ventricular tissue after induction of 2 weeks aortic insuffiency and subsequently 16 weeks of banding (**B, D, F**). Re-expression of αSKA and presence of glycogen accumulation in the same areas of pressure and volume overloaded myocardium is evident. Scale bars represent 20 μm.

by the development of αCA stress fibres in a fan-like distribution pattern in the spreading processes (Group 2, Fig. 4C). As the dedifferentiation process continued, the spreading with αCA-positive stress fibres progressed towards the lateral sides of the cell (Group 3, Fig. 4D). Electron microscopy showed a gradual loss of sarcomeric myofilaments (Figs. 4E and 6A) and the occurrence of stress fibres in the spreading areas with residual actin filaments still visible (Fig. 4E). The complete spreading of the outer plasma membrane was accompanied by stress fibres all over the outer surface; remnants of the sarcomeric structure of the myofibrils were still present at the centre of the cell (Group 4, Fig. 4F). Finally, the cardiomyocytes showed a rounded appearance with only a myofibrilar core remaining (Group 5, Fig. 4G). The time course for fully progressed dedifferentiation in culture covered at least 4 days.

No αSKA expression was seen at the distal ends of freshly isolated cardiomyocytes after 3 hrs of culture. As soon as the cardiomyocytes started differentiation after 1 day in co-culture αSKA expression became visible at the rounded distal ends (Group 1 cells, Fig. 5A). The expression progressively and specifically increased upon further differentiation. As such, the expression of αSKA was observed in the cytoplasmic processes at the distal ends after 2 days (Group 2, Fig. 5B) and was progressively seen in the spreadings at the lateral sides of the cardiomyocytes (Group 3 and 4, Fig. 5C and E) mainly after 3 and 4 days in co-culture, respectively. αSKA co-localized with the developing αCA stress fibres (Fig. 5D) and was characterized by a rather patchy staining pattern. Upon further dedifferentiation, the rounded cardiomy-

ocytes showed a punctate αSKA positivity throughout the entire cytoplasm mainly after 4 days in co-culture (Group 4 and 5, Fig. 5E and F).

Chronic atrial fibrillation in goats

Atrial cardiomyocytes from goats in sinus rhythm showed longitudinal myofibres with a regular pattern of sarcomeres throughout the cytoplasm with parallel rows of mitochondria and the presence of some distributed glycogen granules (Fig. 6B and C). During 4 weeks of AF, structural remodelling of the cardiomyocytes was observed, characterized by gradual disruption of the sarcomeric apparatus or myolysis and a concomitant accumulation of glycogen (Fig. 6D). After 16 weeks of AF, the majority of the myofilaments have been replaced by large glycogen accumulations (Fig. 6E) as verified, in addition, by PAS staining (Fig. 6F).

Transverse sections of right atrial myocardium from goats in sinus rhythm showed intense αCA staining in all cardiomyocytes (Fig. 7A and Table 2). In adjacent serial sections, only very limited αSKA staining (<1% of total tissue area) (Fig. 7B) and no glycogen accumulation could be detected, as verified by PAS staining (Fig. 7C). After 1 week of AF, the αCA expression was unaltered (Fig. 7D) but several areas of atrial muscle tissue displayed an intense patchy staining of αSKA (15% of total tissue area) in the cytoplasm of cardiomyocytes (Fig. 7E). PAS staining of the same regions revealed a minor degree of glycogen deposition (Fig. 7F).
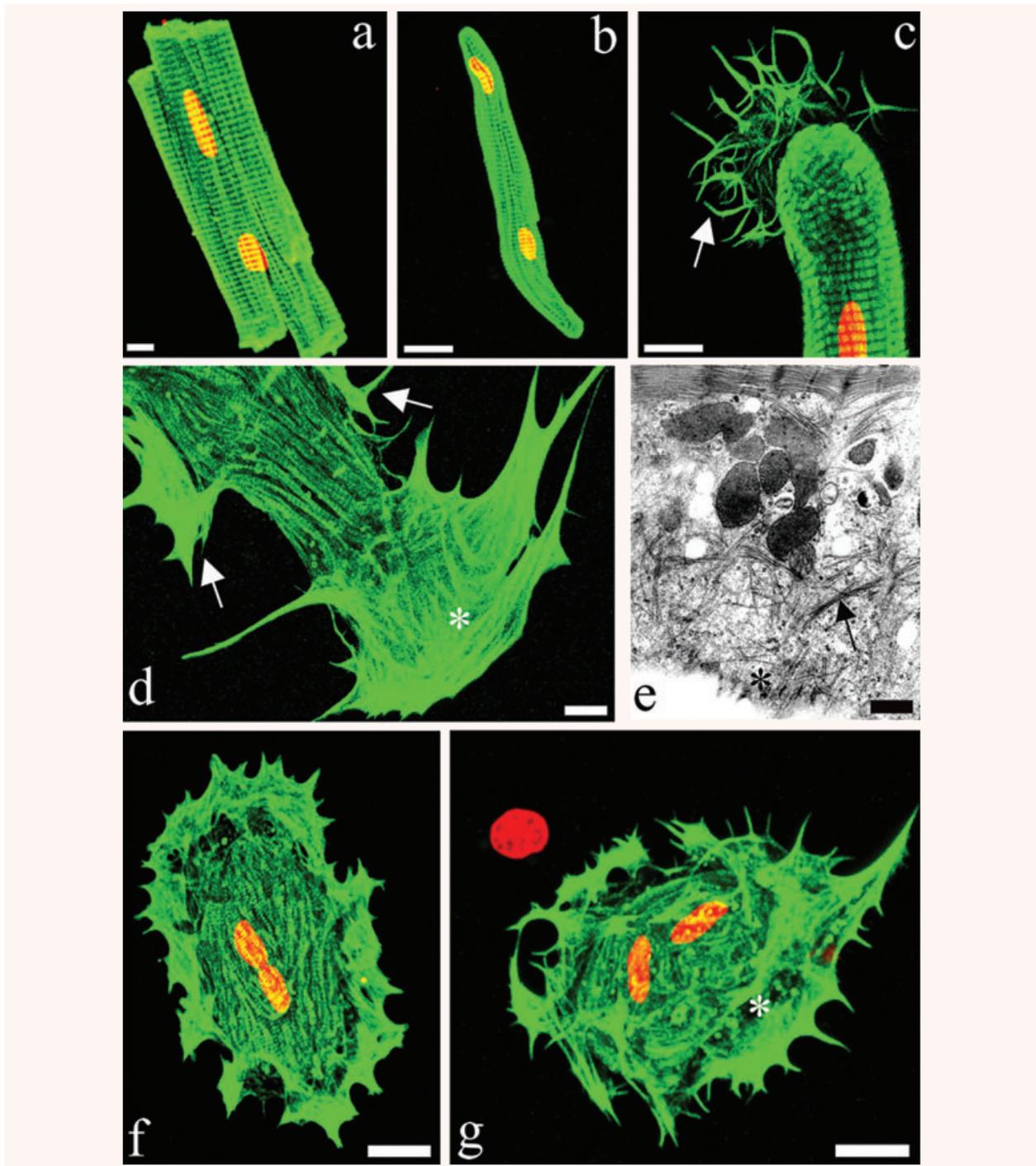
Fig. 4 Immunofluorescence imaging of αCA (**A, B, C, D, F, G**) and electron microscopy (**E**) of (**A**) freshly isolated rectangular rabbit cardiomyocytes, (**B**) Group 1, (**C**) Group 2, (**D, E**) Group 3, (**F**) Group 4 and (**G**) Group 5 CMs. Arrows in (**C**) and (**D**) point to the distal and lateral protrusions, respectively. * indicates the localization of actin stress fibres (**D, E, G**). PI counterstaining of nuclei in red. Scale bars represent 20 μm (**A, B, F, G**), 10 μm (**C** and **D**) and 500 nm (**E**).
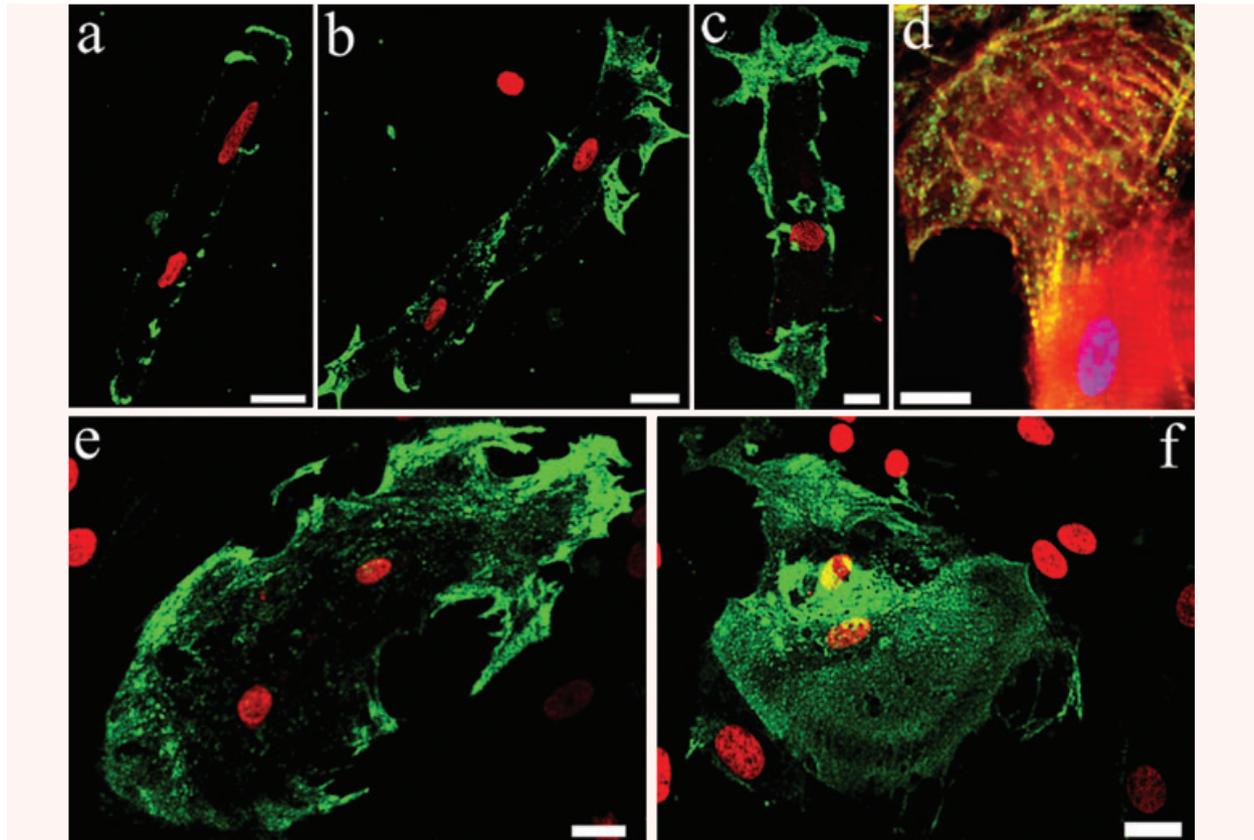
Fig. 5 Immunofluorescence imaging of αSKA re-expression in cardiomyocytes of (**A**) Group 1, (**B, D**) Group 2, (**C**) Group 3, (**E**) Group 4 and (**F**) Group 5 CMs. (**D**) Co-localization of actin stress fibres and αSKA expression. PI (**A, B, C, E, F**, red) and DAPI (**D**, blue) counterstaining of nuclei. Scale bars represent 10 μm (**D**) and 20 μm (**A, B, C, E, F**).

In the weeks following these initial changes, a gradual increase in glycogen deposition was observed in αSKA-positive cardiomyocytes (Table 2). After 16 weeks of AF, patchy staining of αSKA in the cytoplasm (25% of total tissue area) could be observed (Fig. 7G and J). PAS staining of the corresponding myocytes often showed intense pink deposits, indicating obvious amounts of glycogen (Fig. 7H and K). However, not all cardiomyocytes accumulating large amounts of PAS-positive glycogen showed also αSKA staining. Cross-striated αCA staining remained present as observed in the longitudinal sections (Fig. 7I).

Discussion

In this study, we investigated the re-expression of the sarcomeric αSKA protein in different pathological models characterized by cardiomyocyte dedifferentiation and compared the *in vivo* setting to that of adult ventricular cardiomyocytes in culture.

In patients suffering from coronary stenosis, we have found an up-regulation of αSKA in hibernating cardiomyocytes with a decreased expression of αCA and cardiotin. Down-regulation of mitochondrial associated cardiotin [26] has previously been described as an early marker for dedifferentiation in the same human samples [22, Table 1] and in several animal models of hibernating myocardium [17, 18, 33]. Abundant expression of αCA and cardiotin was found in non-hibernating regions showing only minor expression of αSKA. This diffuse αSKA expression can be explained by previous studies reporting the age-dependent up-regulation of αSKA expression increasing steadily during development and after birth, becoming a predominant isoform in adult cardiomyocytes [5] and the localization of αSKA-positive cardiomyocytes as a transmural gradient mainly in the subendocardial part of the adult human heart [7]. Another possibility might be that the αSKA-positive cardiomyocytes were in a stage of hypertrophy thereby expressing αSKA. The absence of αSKA observed in αCA and cardiotin-negative cardiomyocytes points to an advanced stage of hibernation, which is characterized by a high degree of myolysis [22, Table 1]. Furthermore, co-expression of
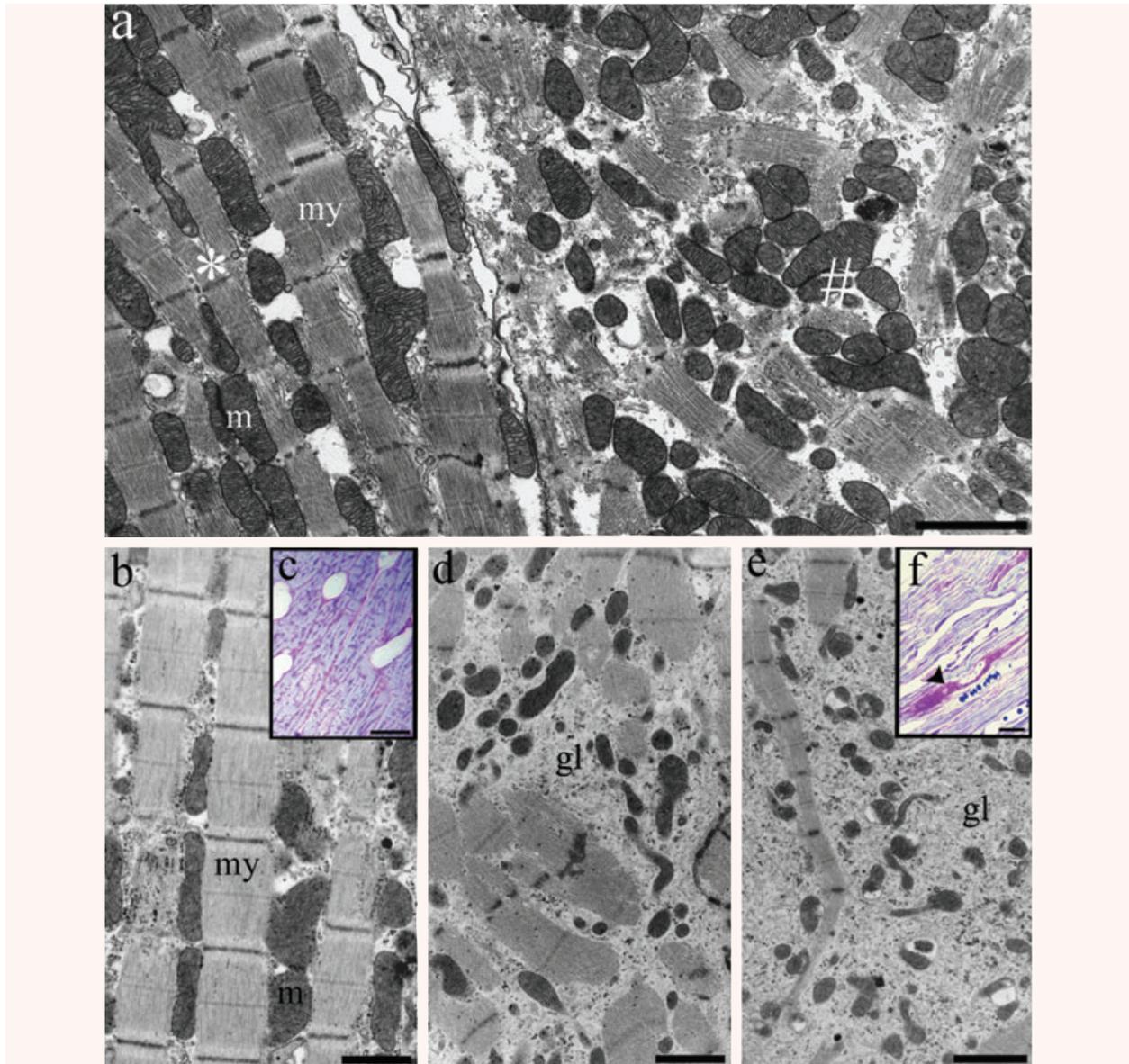
Fig. 6 Electron microscopy of isolated rabbit ventricular cardiomyocytes after 4 days in culture (**A**) and goat atrial tissue in sinus rhythm (**B, C**), after 4 weeks (**D**) and 16 weeks of chronic atrial fibrillation (**E, F**). (**A**) Cultured ventricular cardiomyocyte (*) showing intact myofilaments (my) with longitudinal rows of mitochondria (**M**) and a dedifferentiating cardiomyocyte (#) with obvious disruption of the sarcomeric apparatus. Atrial cardiomyocytes in sinus rhythm (**B**) show well-organized myofilaments (my) with parallel rows of mitochondria (**M**) and absence of glycogen accumulation. Periodic acid Schiff (PAS) staining revealed no glycogen in the cardiomyocytes, as evaluated by light microscopy (**C**). Gradual disruption of myofilaments is observed during 4 (**D**) and 16 weeks of AF (**E**) and is associated with apparent glycogen accumulation (gl). The glycogen stores are clearly seen after PAS staining (**F**, arrowhead). Scale bars represent 1 μm (**B, D**), 2 μm (**A, E**) and 15 μm (**C, F**).

αSKA and glycogen was observed in cardiomyocytes from left ventricles of rabbit hearts suffering from pressure- and volume-overload. However, only a limited number of glycogen-positive cells were found suggesting that the myocytes were in a rather early stage of dedifferentiation and/or myolysis.

Cultured adult rabbit ventricular cardiomyocytes serve as a valuable experimental model to address some important questions that are relevant to the structural changes seen during cardiomyocyte dedifferentiation. The changes in ultrastructure and expression patterns of structural proteins exhibit similarities with
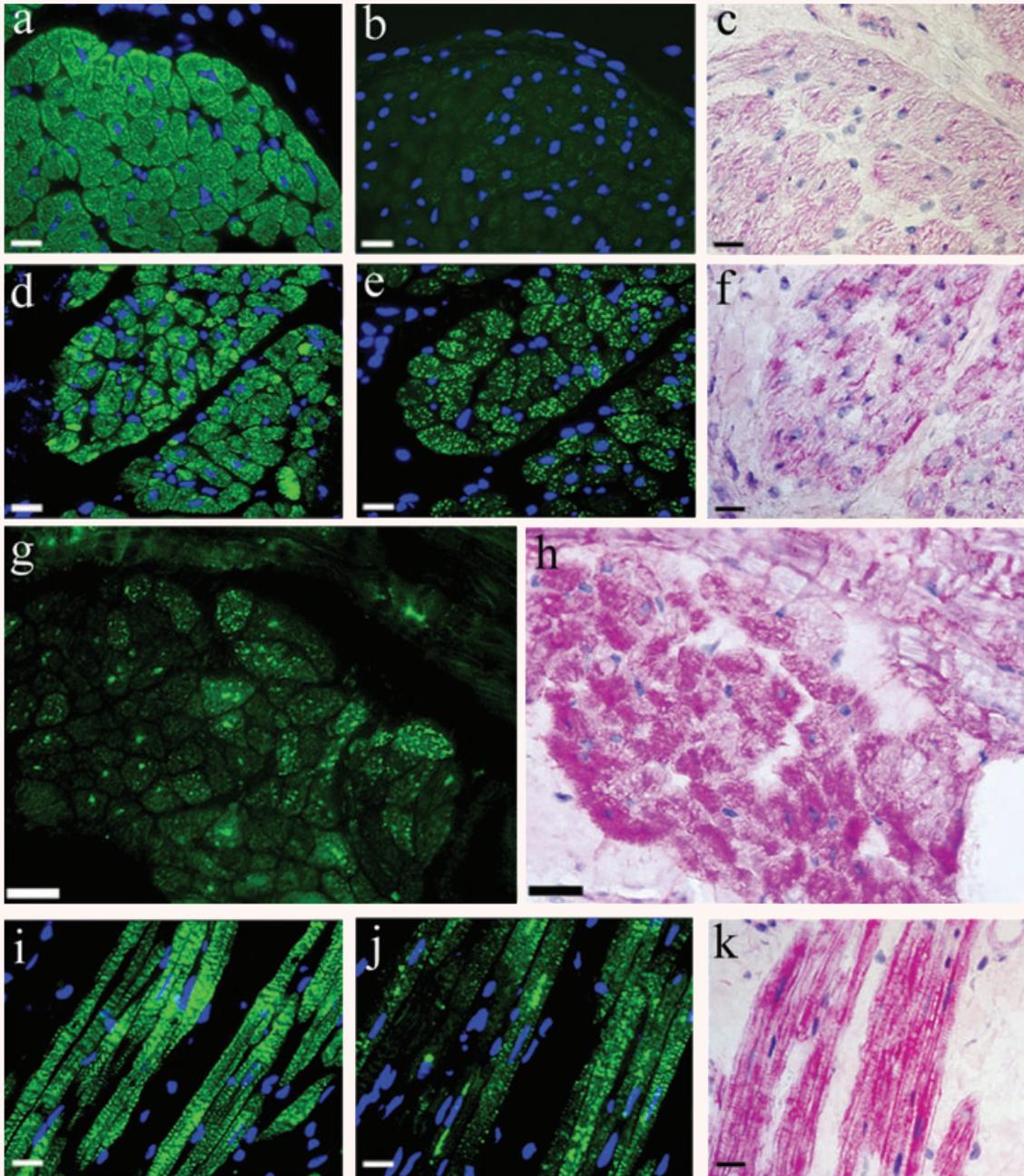
Fig. 7 Detection of αCA (**A, D, I**), αSKA (**B, E, G, J**) and periodic acid Schiff (PAS)-positive glycogen (**C, F, H, K**) on serially frozen sections from a normal goat atrium in sinus rhythm (**A, B, C**) and after 1 week (**D, E, F**) and 16 weeks (**G, H, I, J, K**) of chronic atrial fibrillation. The absence of αSKA expression and glycogen accumulation in sinus rhythm, on the one hand, and re-expression of αSKA and glycogen staining in goat atrial fibrillation, on the other hand, is evident. Scale bars represent 20 μm.

hibernating cardiomyocytes *in vivo* [34]. Previously, we have sub-divided this process of structural adaptation into five successive morphological steps [32]. The remodelling started at the distal end of the cardiomyocyte through the disassembly of the interca-lated disk and the formation of cytoplasmic processes. These cytoplasmic processes progressively extended over the whole plasma membrane and caused progressive morphological changes of the cardiomyocytes from a highly organized cylinder to a fully flattened cell. Spreading of the cardiomyocytes is charac-terized by a progressive disruption of the sarcomeric organization leaving only remnants of αCA-containing thin filaments in the myolytic regions.

Our study now revealed that the spreading of the plasma mem-branes coincided with the development of αCA stress fibres in the posterior protrusions, which progressed towards the lateral sides of the cells. Peripheral stress fibres attached to membranous ruf-fles, which are positive for α-actin, have earlier been described in the pseudopods of embryonic chick cardiomyocytes. These were shown to interconnect with fine polygonal networks located between developing myofibrils [35]. Furthermore, the formation of actin stress fibres containing αSMA was observed in filopodia of spreading adult rat cardiomyocytes in culture [36, 37]. It has been postulated that during myofibrillogenesis, α-actin containing stress fibres can serve as a scaffold to direct the assembly of nascent striated myofilaments, which disappear as the myofila-ments mature [1, 38]. This was evidenced in remodelled adult rat cardiomyocytes in culture after the administration of insulin-like growth factor I, which stimulated myofilament development in the filopodia and caused a down-regulation of the non-sarcomeric αSMA [35, 39]. In our study, we have demonstrated the re-expression of αSKA in posterior and lateral protrusions that contain αCA stress fibres, and observed also an increased punc-tate staining towards the centre of the cell in later stages of dedif-ferentiation. A similar phenomenon was seen in cultured quail embryonic fibroblasts treated with metabolic inhibitors that caused the disassembly of all types of actin structures [40]. After removal of the inhibitors, restoration of the actin cytoskeleton at the edges of the fibroblasts was observed. This was characterized by actin polymerization at the cell periphery gradually expanding towards the centre of the cell. The punctate αSKA staining pattern in our cardiomyocytes was similar to that seen in the tissue sec-tions of the rabbit model of pressure- and volume-overloaded myocardium. A chronology of αSKA incorporation within the sar-comeres after cardiomyocyte spreading was suggested by Clément *et al.* [41], starting from punctate aggregates similar to those described for other components of myofibrils, such as α-actinin forming 'Z-bodies' [42–44], followed by an incorporation into actin stress fibres, which in turn could serve as templates for myofibrils [45]. Contrary to adult rat cardiomyocytes in long-term culture, which have the ability to generate new myofibrillar struc-tures [46], no reassembly of myofilaments was observed in our co-culture setting. Furthermore, the co-culture system shares a common denominator with the aforementioned cardiovascular pathologies in that high levels of passive load or stretch are imposed onto the cardiomyocytes resulting in gradual disruption

Table 1 Time-related expression of proteins in human hibernating ven-tricular myocardium

Protein	Time-period of hibernating myocardium		
	Normal myocardium	Early changes	Late changes
α cardiac actin	+	+	+/−
α skeletal actin	−	+	+/−
α smooth muscle actin [22]	−	−	+
Glycogen [19, 22]	−	±	+
Cardiotin [22]	+	−	−

Table 2 Time-related expression of proteins during atrial fibrillation

Protein	Time-period of atrial fibrillation (weeks)					
	0	1	2	4	8	16
α cardiac actin	+	+	+	+	+	+
α skeletal actin	−	+	+	+	+	+
α smooth muscle actin [17]	−	±	±	±	+	+
Glycogen	−	±	±	+	+	+
Cardiotin [17]	+	±	±	−	−	−

of the sarcomeric apparatus [32]. This phenomenon has also been observed in the chronic AF goat set up, which is regarded as a highly suitable model to study dedifferentiation of atrial myocytes resembling chronic hibernating myocardium of the ventricle. High-resolution electron microscopy performed as early as 1 week after AF indicated a homogeneous redistribution of heterochro-matin throughout the cardiomyocyte nuclei. The first signs of myolysis and glycogen accumulation occurred after 1–2 weeks of AF. Thereafter, progressive stages of dedifferentiation were identified at 4 and 16 weeks of AF showing gradual increase in glycogen accumulation, myolysis, alterations of the mitochondrial morphol-ogy and a disorganization of the sarcoplasmic reticulum. These ultrastructural changes, which have been extensively described in a previous study [17], are highly comparable with the myolytic events identified in our cardiomyocyte culture system.

Therefore, we performed alpha-sarcomeric actin immunostain-ings on the same samples used in the previous study and com-pared it to the described αSMA expression [17] at the same time intervals. We did not find significant variations in αCA expression between normal and pathological samples during 16 weeks of AF. However, from 1 week of AF onwards an obvious re-expression of αSKA was seen in some regions of the atrial myocardium, with similar expression patterns being found during the subsequent 16 weeks of AF. Glycogen accumulation also gradually increased in

the αSKA-positive cardiomyocytes. A gradual re-expression of αSMA from 2 weeks of AF onwards has been described earlier to result in increased staining after 8 weeks and 16 weeks [17]. Restoration of the sinus rhythm after 16 weeks of AF caused a slow recovery from the structural remodelling and was accompanied by a decrease in αSMA positivity from 4 months post-AF onwards [47]. The re-expression of αSMA in cardiomyocytes with a hibernating phenotype has also been observed in the left atrial posterior wall of human patients with chronic AF [48]. Our data combined with previous results suggest a reverse myofibrillogenesis process as indicated by the time-related re-expression of αSKA followed by that of αSMA (see Table 2). The αSKA positivity in AF occurred only as diffuse aggregates without any structural organization into striated myofilaments and is similar to the staining patterns observed in dedifferentiating ventricular cardiomyocytes *in vitro* and *in vivo*. Since the reactivation of the foetal cardiac gene program is also a characteristic feature of hypertrophic cardiomyocytes during heart failure, the main distinction between hypertrophy and hibernation under these conditions was made by the presence or absence of glycogen accumulation in the respective pathologies [49]. The reason why in the goat model also cardiomyocytes could be observed containing large amounts of glycogen without expression of αSKA may be that these cells were possibly in an end stage of dedifferentiation and thereby had lost αSKA expression.

The presence of multiple α-actins appears to provide a diversity in contractile properties that may be related to the physiological demand at the level of the cell and tissue. A mutation in the αCA gene of BALB/c adult mice revealed a correlation between the relative actin isoform content and cardiac function. Increased disassembly of αCA-positive sarcomeres was compensated by elevated expression of αSKA and increased contractile function [50]. αSKA up-regulation in dedifferentiating cardiomyocytes can therefore be regarded as an adaptation mechanism towards the impaired contractile function and could serve as a scaffold for rebuilding the sarcomeric structures during myofibrillogenesis.

Restoration of the blood flow by coronary artery bypass surgery offers hibernating myocardium the opportunity to restore its contractile function [22, 51]. However, there is often a delayed recovery ascribed to the increased interstitial tissue or to the far advanced stage of myolysis of the sarcomeric apparatus [52]. Due to the early expression of αSKA, it can be hypothesized that the level of αSKA is a useful determinant for the degree of dedifferentiation in hibernating myocardium and an indicator for possible redifferentiation.

Our results on αSKA re-expression in the myocardial dedifferentiation models invite for further research into the mechanisms regulating actin isoform expression and can contribute to the additional understanding of myofilament assembly during myofibrillogenesis.

Acknowledgements

References

1. **Vandekerckhove J, Bugaisky G, Buckingham M.** Simultaneous expression of skeletal muscle and heart actin proteins in various striated muscle tissues and cells. *J Biol Chem*. 1986; 261: 1838–43.

2. **Vandekerckhove J, Weber K.** At least six different actins are expressed in a higher mammal: an analysis based on the amino acid sequence of the amino-terminal tryptic peptide. *J Mol Biol*. 1978; 126: 783–802.

3. **Ruzicka DL, Schwartz RJ.** Sequential activation of α-actin genes during avian cardiogenesis: vascular smooth muscle α-actin gene transcripts mark the onset of cardiomyocyte differentiation. *J Cell Biol*. 1988; 107: 2575–86.

4. **Boheler KR, Carrier L, de la Bastie D, Allen PD, Komajda M, Mercadier JJ, Schwartz K**. Skeletal actin mRNA increases in the human heart during ontogenic development and is the major isoform of control and failing adult hearts. *J Clin Invest*. 1991; 88: 323–30.

5. **Carrier L, Boheler KR, Chassagne C, de la Bastie D, Wisnewsky C, Lakatta EG.** Expression of the sarcomeric actin isogenes in the rat heart with development and senescence. *Circ Res*. 1992; 70: 999–1005.

6. **Suurmeijer AJH, Clément S, Francesconi A, Bocchi L, Angelini A, Van Veldhuizen J, Spagnoli LG, Gabbiani G, Orlandi A.** α-Actin isoform distribution in normal and failing human heart: a morphological, morphometric, and biochemical study. *J Pathol*. 2003; 199: 387–97.

7. **Clément S, Stouffs M, Bettiol E, Kampf S, Krause K-H, Chaponnier C, Jaconi M.** Expression and function of α-smooth muscle actin during embryonic-stem-cell-derived cardiomyocyte differentiation. *J Cell Sci*. 2007; 120: 229–38.

8. **Chaponnier C, Gabbiani G.** Pathological situations characterized by altered actin isoform expression. *J Pathol*. 2004; 204: 386–95.

9. **Schwartz K, de la Bastie D, Bouveret P, Oliviéro P, Alonso S, Buckingham M.** α-Skeletal muscle m-RNA's accumulate in hypertrophied adult rat hearts. *Circ Res*. 1986; 59: 551–5.

10. **Winegrad S, Wisnewsky C, Schwartz K.** Effect of thyroid hormone on the accumulation of mRNA for skeletal and cardiac α-actin in hearts from normal and hypophysectomized rats. *Proc Natl Acad Sci USA*. 1990; 87: 2456–60.

11. **Clément S, Chaponnier C, Gabbiani G.** A subpopulation of cardiomyocytes expressing α-skeletal actin is identified by a specific polyclonal antibody. *Circ Res*. 1999; 85: e51–8.

12. **Stilli D, Bocchi L, Berni R, Zaniboni M, Cacciani F, Chaponnier C, Musso E, Gabbiani G, Clément S.** Correlation of α-skeletal actin expression, ventricular fibrosis and heart function with the degree of pressure overload cardiac hypertrophy in rats. *Exp Physiol*. 2006; 91: 571–80.

13. **Izumo S, Nadal-Ginard B, Mahdavi V.** Protooncogene induction and reprogramming of cardiac gene expression produced

by pressure overload. *Proc Natl Acad Sci USA*. 1988; 85: 339–43.

14. **Komuro I, Katoh Y, Kaida T, Shibazaki Y, Kurabayashi M, Hoh E, Takaku F, Yazaki Y.** Mechanical loading stimulates cell hypertrophy and specific gene expression in cultured rat cardiac myocytes. *J Biol Chem*. 1991; 266: 1265–8.

15. **Bishopric NH, Simpson PC, Ordahl CP.** Induction of the skeletal α-actin gene in α1-adrenoceptor-mediated hypertrophy of rat cardiac myocytes. *J Clin Invest*. 1987; 80: 1194–9.

16. **Parker TG, Chow KL, Schwartz RJ, Schneider MD.** Differential regulation of skeletal α-actin transcription in cardiac muscle by two fibroblast growth factors. *Proc Natl Acad Sci USA*. 1990; 87: 7066–70.

17. **Ausma J, Litjens N, Lenders MH, Duimel H, Mast F, Wouters L, Ramaekers F, Allessie M, Borgers M.** Time course of atrial fibrillation-induced cellular structural remodeling in atria of the goat. *J Mol Cell Cardiol*. 2001; 33: 2083–94.

18. **Dispersyn GD, Mesotten L, Meuris B, Maes A, Mortelmans L, Flameng W, Ramaekers F, Borgers M.** Dissociation of cardiomyocyte apoptosis and dedifferentiation in infarct border zones. *Eur Heart J*. 2002; 23: 849–957.

19. **Borgers M, Thoné F, Wouters L, Ausma J, Shivalkar B, Flameng W.** Structural correlates of regional myocardial dysfunction in patients with critical coronary artery stenosis: chronic hibernation? *Cardiovasc Pathol*. 1993; 2: 237–45.

20. **Maes A, Flameng W, Nuyts J, Borgers M, Shivalkar B, Ausma J, Bormans G, Schiepers C, De Roo M, Mortelmans L.** Histological alterations in chronically hypoperfused myocardium. Correlation with PET findings. *Circulation*. 1994; 90: 735–45.

21. **Vanoverschelde JL, Wijns W, Borgers M, Heyndrickx G, Depré C, Flameng W, Melin JA.** Chronic myocardial hibernation in humans. From bedside to bench. *Circulation*. 1997; 95: 1961–71.

22. **Ausma J, Schaart G, Thoné F, Shivalkar B, Flameng W, Depré C, Vanoverschelde JL, Ramaekers F, Borgers M.** Chronic ischemic viable myocardium in man: aspects of dedifferentiation. *Cardiovasc Pathol*. 1995; 4: 29–37.

23. **Sharov VG, Sabbah HN, Ali AS, Shimoyama H, Lesch M, Goldstein S.** Abnormalities of cardiocytes in regions bordering fibrous scars of dogs with heart failure. *Int J Cardiol*. 1997; 60: 273–9.

24. **Dispersyn GD, Ausma J, Thoné F, Flameng W, Vanoverschelde J, Allessie MA, Ramaekers FC, Borgers M.** Chronic hibernating myocardium and chronic atrial fibrillation: a prelude to apoptosis? *Cardiovasc Res*. 1999; 43: 947–57.

25. **Kilpatrick KE, Wring SA, Walker DH, Macklin MD, Payne JA, Su JL, Champion BR, Caterson B, McIntyre GD.** Rapid development of affinity matured monoclonal antibodies using RIMMS. *Hybridoma*. 1997; 16: 381–9.

26. **Driesen RB, Verheyen FK, Schaart G, de Mazière A, Viebahn C, Prinzen FW, Lenders MH, Debie W, Totzeck A, Borgers M, Ramaekers FCS.** Cardiotin localization in mitochondria of cardiomyocytes *in vivo* and *in vitro* and its downregulation during dedifferentiation. Doi:10.1016/j.carpath .2007.12.008

27. **Schaart G, van der Ven PFM, Ramaekers FCS.** Characterization of cardiotin, a structural component in the myocard. *Eur J Cell Biol*. 1993; 62: 34–48.

28. **Schaart G, Moens L, Endert JM, Ramaekers FCS.** Biochemical characterization of cardiotin, a sarcoplasmic reticulum associated protein. *FEBS Lett*. 1997; 403: 168–72.

29. **Vermeulen JT, McGuire MA, Opthof T, Coronel R, de Bakker JM, Klopping C.** Triggered activity and automaticity in ventricular trabeculae of failing human and rabbit hearts. *Cardiovasc Res*. 1994; 28: 1547–54.

30. **Wijffels MCEF, Kirchhof CJMJ, Dorland R, Allessie MA.** Atrial fibrillation begets atrial fibrillation. *Circulation*. 1995; 92: 1954–68.

31. **Driesen RB, Dispersyn GD, Verheyen FK, van den Eijnde SM, Hofstra L, Thoné F, Dijkstra P, Debie W, Borgers M, Ramaekers FC.** Partial cell fusion: a newly recognized type of communication between dedifferentiating cardiomyocytes and fibroblasts. *Cardiovasc Res*. 2005; 68: 37–46.

32. **Driesen RB, Verheyen FK, Dispersyn GD, Thoné F, Lenders MH, Ramaekers FCS, Borgers M.** Structural adaptation in adult rabbit ventricular myocytes. Influence of dynamic physical interaction with fibroblasts. *Cell Biochem Biophys*. 2006; 44: 119–28.

33. **Thijssen VLJL, Borgers M, Lenders MH, Ramaekers FCS, Suzuki G, Palka B, Fallavollita JA, Thomas SA, Canty JM Jr.** Temporal and spatial variations in structural protein expression during the progression from stunned to hibernating myocardium. *Circulation*. 2004; 110: 3313–21.

34. **Dispersyn GD, Geuens E, Ver Donck L, Ramaekers FCS, Borgers M.** Adult rabbit cardiomyocytes undergo hibernation-like dedifferentiation when co-cultured with cardiac fibroblasts. *Cardiovasc Res*. 2001; 51: 230–40.

35. **Wang S, Greaser ML, Schultz E, Bulinski JC, Lin J, Lessard JL.** Studies on cardiac myofibrillogenesis with antibodies to titin, actin, tropomyosin and myosin. *J Cell Biol*. 1988; 107: 1075–83.

36. **Eppenberger-Eberhardt M, Flamme I, Kurer V, Eppenberger HM.** Reexpression of α-smooth muscle actin isoform in cultured adult rat cardiomyocytes. *Dev Biol*. 1990; 139: 269–78.

37. **Donath MY, Zapf J, Eppenberger-Eberhardt M, Froesch R, Eppenberger H.** Insulin-like growth factor I stimulates myofibril development and decreases smooth muscle α-actin of adult cardiomyocytes. *Proc Natl Acad Sci USA*. 1994; 91: 1686–90.

38. **Dlugosz A, Antin PB, Nachmias VT, Holtzer H.** The relationship between stress fiber-like structures and nascent myofibrils in cultured cardiac myocytes. *J Cell Biol*. 1984; 99: 2268–78.

39. **Harder BA, Schaub MC, Eppenberger HM, Eppenberger-Eberhardt M.** Influence of fibroblast growth factor (bFGF) and insulin-like growth factor (IGF-I) on cytoskeletal and contractile structures and on atrial natriuretic factor (ANF) expression in adult rat ventricular cardiomyocytes in culture. *J Mol Cell Cardiol*. 1996; 28: 19–31.

40. **Svitkina TM, Neyfakh AA.** Actin cytoskeleton of spread fibroblasts appear to assemble at the cell edges. *J Cell Sci*. 1986; 82: 235–48.

41. **Clément S, Pellieux C, Chaponnier C, Pedrazzini T, Gabbiani G.** Angiotensin II stimulates α-skeletal actin expression in cardiomyocytes *in vitro* and *in vivo* in the absence of hypertension. *Differentiation*. 2001; 69: 66–74.

42. **Rhee D, Sanger JM, Sanger JW.** The premyofibril: evidence for its role in myofibrillogenesis. *Cell Motil Cytoskeleton*. 1994; 28: 1–24.

43. **Dabiri GA, Turnacioglu KK, Sanger JM, Sanger JW.** Myofibrillogenesis visualized in living embryonic cardiomyocytes. *Proc Natl Acad Sci USA*. 1997; 94: 9493–8.

44. **Carroll SL, Horowits R.** Myofibrillogenesis and formation of cell contacts mediate the localization of N-RAP in cultured chick

cardiomyocytes. *Cell Motil Cytoskeleton.* 2000; 47: 63–76.

45. **Bershadsky AD, Glück U, Denisenko ON, Sklyarova TV, Spector I, Ben-Ze'ev A.** The state of actin assembly regulates actin and vinculin expression by a feedback loop. *J Cell Sci.* 1995; 108: 1183–93.

46. **Eppenberger ME, Hauser I, Baechi T, Schaub MC, Brunner UT, Dechesne CA, Eppenberger HM.** Immunocytochemical analysis of the regeneration of myofibrils in long-term cultures of adult cardiomyocytes of the rat. *Dev Biol.* 1988; 130: 1–15.

47. A**usma J, van der Velden HMW, Lenders M-H, van Ankeren EP, Ramaekers FCS, Borgers M, Allessie MA.** Reverse structural and gap-junctional remodelling after prolonged atrial fibrillation in the goat. *Circulation.* 2003; 107: 2051–8.

48. **Corradi D, Callegari S, Benussi S, Maestri R, Pastori P, Nascimbene S, Bosio S, Dorigo E, Grassani C, Rusconi R, Vettori MV, Alinovi R, Astorri E, Pappone C, Alfieri O.** Myocyte changes and their left atrial distribution in patients with chronic atrial fibrillation related to mitral valve disease. *Hum Pathol.* 2005; 36: 1080–9.

49. **Vernooy K, Verbeek XAAM, Peschar M, Crijns HJGM, Arts T, Cornelussen RNM, Prinzen FW.** Left bundle branch block induces ventricular remodelling and functional septal hypoperfusion. *Eur Heart J.* 2005; 26: 91–8.

50. **Hewett TE, Grupp IL, Grupp G, Robbins J.** Alpha skeletal actin is associated with increased contractility in the mouse heart. *Circ Res.* 1994; 74: 740–6.

51. **Tubau JF, Rahimtoola SH.** Hibernating myocardium: a historical perspective. *Cardiovasc Drugs Ther.* 1992; 6: 267–71.

52. **Ausma J, Cleutjens J, Thoné F, Flameng W, Ramaekers F, Borgers M.** Chronic hibernating myocardium: interstitial changes. *Mol Cell Biochem.* 1995; 147: 35–42.